FE MODELING OF PARTICULATE COMPOSITES WITH BRITTLE MATRIX UNDER CYCLIC COMPRESSION LOADING

J. HEGER, M. KOTOUL AND T. VYSLOUŽIL

Department of Solid Mechanics, Technical University of Brno, Technická 2, 616 69 Brno, Czech Republic

ABSTRACT

Finite element analysis was attempted to modeling of overall response of metal particulate-reinforced brittle matrix composites under cyclic loading. The aim was to make comparison with the predictions of micromechanical averaging model exposed in an accompanying paper in the proceedings [1]. A random material microgeometry of the composite was replaced with a certain periodic approximation and a unit cell was selected for evaluation of the local fields and the overall response. Stress-strain analysis of the ductile inclusion in brittle matrix was performed using the program system ANSYS. The weakening constraint of the matrix caused by microfracture damage around inclusions was carefully modeled and its impact upon the overall response of the composite was investigated.

KEYWORDS

Finite element method, Low Cycle Loading, Ceramics, Microfracturing

INTRODUCTION

As already noted in the contribution [1], brittle solids fail by a process of progressive microfracture. If subjected to cyclic loading beyond the elastic range with nonzero mean stress, usually there is a cycle by cycle accumulation of inelastic strain related to microfracturing in the direction of mean stress similarly like an accumulation of plastic strain in metals. This phenomenon is called cyclic creep or ratchetting. A micromechanical model based on Mori-Tanaka's approach was used in [1] to modelling metal particulate-reinforced brittle matrix composites under cyclic compression loading. It was shown that the weakening constraint of the matrix caused by microcracks nucleated in the matrix from the inclusion's poles, as a consequence of a local concentrated tensile field, is closely coupled with the plasticity of ductile inclusions and leads to ratchetting even when the plastic deformation of inclusions is described by an isotropic hardening rule. The fact, that the isotropic hardening rule for inclusions together with matrix microcracking can lead to ratchetting of composite, is rather surprising because it is well known from the cyclic plasticity of metals that models capable to predict ratchetting require a special kind of kinematic translation rule containing the dynamic recovery term. However, it was proved in [1] that the suggested micromechanical model possesses the same mathematical structure on the macroscopic level as the phenomenological J_2- flow theory with the mentioned kinematic hardening rule, which explains the observed model behaviour.

It is a matter of interest to check, at least qualitatively, the micromechanical model behaviour using finite element analysis. To do so, a random material microgeometry of metal particulate-reinforced brittle matrix composite must be replaced with a certain periodic approximation together with a unit cell selection due to computational purposes. Of course, this crude approximation inhibits to perform quantitative comparisons, but still enables us to find out, whether the ratchetting phenomenon is unambiguously related to the presence of microcracks stemming from the inclusion's poles.

CALCULATION MODEL

Particulate-reinforced brittle matrix composite studied here is ideal and the inclusions are assumed to be spherical and to be uniformly dispersed in the matrix. This allows resorting to a periodic array model. Specifically, square array was considered. Under overall uniform fields the local fields possess certain symmetric features such that a unit cell can be selected for evaluation of the local fields and the overall response. Finite element interpretation was first created as the plane stress and plane strain 2D model for fibber composites, later as the axis-symmetrical model for particulate composites. Also the more realistic but much more complicated 3D model for particulate composites was created. Mutual comparison proved good results agreement for 2D and 3D cases and confirmed the acceptable preciseness of 2D models.

Utilising 2D models simplicity, numerical modelling of solved problems was performed in the following 5 steps:
1) Linear material properties of the matrix and inclusion considering an ideal connection across their interface.
2) Linear material properties of the matrix and nonlinear material properties of inclusion considering an ideal connection across their interface.
3) Linear material properties of the matrix and inclusion with their possible sliding and debonding at their interface.
4) Linear material properties of the matrix and nonlinear material properties of inclusion with their possible sliding and debonding at their interface.
5) Linear material properties of the matrix and nonlinear material properties of inclusion with their possible sliding and debonding at their interface. Moreover, the crack in the matrix was considered with the length comparable to the inclusion radius and stemming from the inclusion's pole.

At the contact problem solution many test calculations were performed where the influence of friction coefficient and normal stiffness of contact elements on the mutual surface penetration and resulting stress were observed.

The loading was cyclically repeated. In the first load step the pressure of 4800 MPa loaded the upper part of the model. In the second load step the loading was completely removed. This pair of loading steps was repeated until the stress-strain steady state was reached. This is the way that numerical modelling of composite behaviour at cyclic repeated pressure was performed.

According to double symmetry of geometry and loading only one quarter of the unit cell was modelled in 2D cases. Boundary conditions of symmetry were introduced in symmetrical sections. Coupling of displacements was used on the upper loaded surface. It means that the same to all its nodes but unknown displacement in the loading direction was attached. Its unknown value is also the result of the solution. The remaining vertical model wall of the cell was alternatively considered to be restrained or free in the direction perpendicular to the loading direction with coupled but again unknown displacements. The last mentioned alternative proved to be the best description of mutual influencing of the inclusion and matrix.

The scheme of the one quarter of the cell model illustrating the matrix/inclusion configuration together with microcrack originating at the inclusion's pole is shown in Fig. 1.

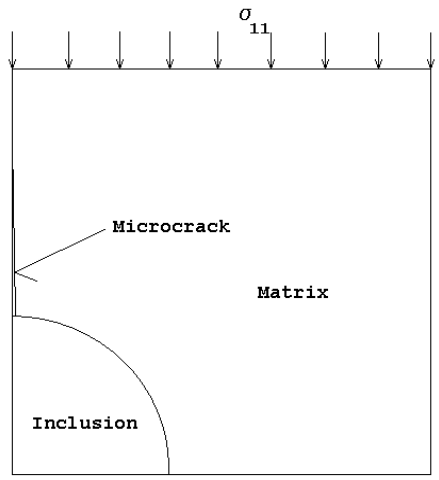

Fig. 1. Scheme of the cell model of one quarter. Loading direction parallel to the principal direction of square array

Meshing of the solved region was consistently performed by the "mapped meshing" technique. All elements in 2D are quadrilaterals, in 3D six sided volumes (bricks). The calculations were performed alternatively with straight sided elements (PLANE42 in 2D and SOLID45 in 3D) and with curved sided elements (PLANE82 in 2D a SOLID95 in 3D). Curved sided elements with midside nodes showed better results and that is why their application was preferred at numerical modelling. Microcrack and the part of the interface around the inclusion's pole, where debonding and sliding can occur as a consequence of microcrack opening, was modelled using contact elements as is schematically shown in Fig. 2.

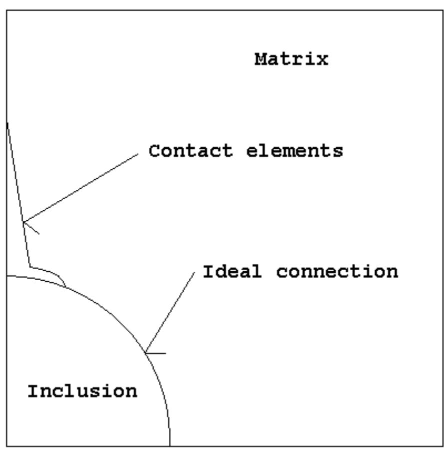

Fig. 2. Microcrack flank and the regions of the matrix/inclusion interface modeled via contact elements

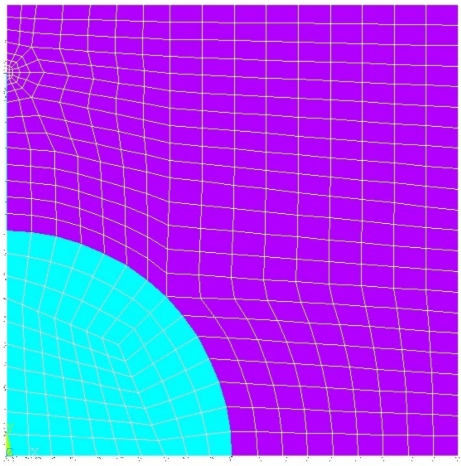

Fig. 3. Sketch of the grid meshing. Microcrack stems from the north pole of the inclusion with refined mesh pertaining to the microcrack tip surroundings

Two patterns of mutual orientation of the inclusion square array arrangement and the compressive loading direction were considered:

1) Model with the loading direction parallel to one of two principal directions of square array,
2) Model with the loading direction containing an angle of 45° with the principal directions of square array.

NUMERICAL RESULTS

All computations were performed for the concentration of inclusions c = 0.2 which, for 2D model, leads to the ratio of the inclusion's diameter over the unit cell size about of 0.504. Besides of the calculation of local strain and stress fields within the unit cell, the calculation of displacement on the upper loaded surface of unit cell became of primary concern. This displacement directly provides an overall strain of unit cell ε_{11} and thus, makes possible to set up an overall stress –strain diagram of composite. Since the main goal of this study is to provide a comparison with the predictions of the micromechanical model suggested in [1], we don't present the results concerning the local fields in the unit cell but do focus only on the overall characteristics such as the accumulation of the permanent overall strain, $\varepsilon_{11,}$ versus number of cycles, N, and the overall stress-strain curve. The following material properties were used in the analysis:

Table 1. Elastic properties of matrix and inclusions

	E	ν
	[MPa]	[-]
Matrix	$7{,}20.10^5$	0,20
Inclusion	$2{,}15.10^5$	0,32

The bilinear curve stress-strain was utilised to model nonlinear dependence in the material of inclusion. Linear behaviour till the stress 1000 MPa was considered in the material of inclusion. Next loading was performed with Young modulus 50 times lower (E = 4300 MPa).

The curve σ - ε was considered symmetrical in both tensile and pressure regions. Such a curve is in a good correspondence with the strain hardening model used in [1].

Results presentation is organised in the following way:

1) the model with the loading direction parallel to the principal direction of square array -
   a) without microcracks,
   b) with microcraks,
2) the model with the loading direction containing an angle of 45° with the principal direction of square array -
   a) without microcracks,
   b) with microcracks.

For each variant it is shown:

i) the accumulation of the permanent overall strain versus number of cycles illustrating if rachetting occurs,
ii) the overall stress-strain curve for first 2 cycles illustrating the overall elastic modulus, the overall yield stress together with the overall hardening rate, and the character of unloading.

Finally, the comparison with predictions of the micromechanical model is made.

Ad 1a)

Fig. 4 indicates that the permanent overall strain accumulates practically in the very first cycle, in accordance with the prediction of the micromechanical model, see [1].

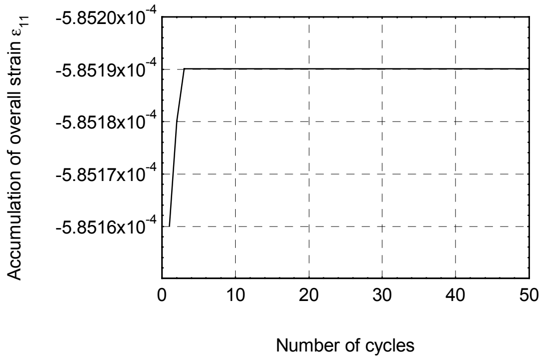

Fig. 4. Accumulation of the permanent overall strain ε_{11}, no microcracking in the matrix

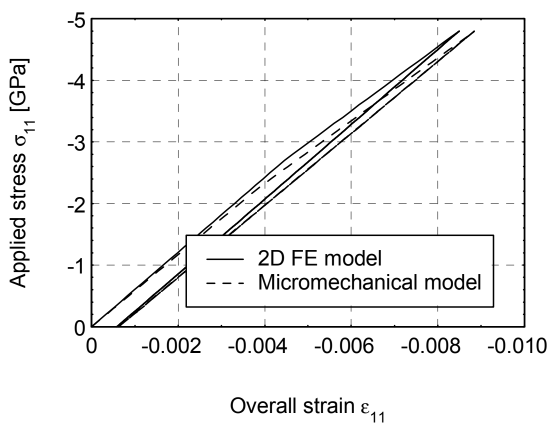

Fig. 5. Predicted overall stress-strain curves, no microcracking in the matrix

Fig. 5 shows the overall stress-strain curves calculated for the first 2 cycles. By comparison with the micromechanical model it follows that the 2D finite element model is somewhat stiffer than the micromechanical model and also predicts higher overall yield stress. Compare the yield stress of inclusion of 1000 MPa with the yield stress of a composite with elastic matrix raising up to 2200 MPa according to the micromechanical model and up to 2600 MPa according to the 2D finite model.

Ad1b)
Fig. 6 shows that in the case of microcrack stemming from the inclusion‘s pole into matrix an accumulation of the permanent overall strain occurs in the first 10 – 30 cycles depending on the range of debonding of the matrix/inclusion interface around the inclusion’s pole, see Fig. 2. Nevertheless, the accumulation of the overall permanent strain is very small comparing to micromechanical model, see [1]. It should be noted that debonding was not modelled within the micromechanical model. Thus a smaller range of debonding is closer to the micromechanical model. Generally, debonding diminishes the permanent overall strain because of the elastic opening of the cracks along the interface, which relaxes residual stresses, and thus partly accommodates the overall permanent strain.

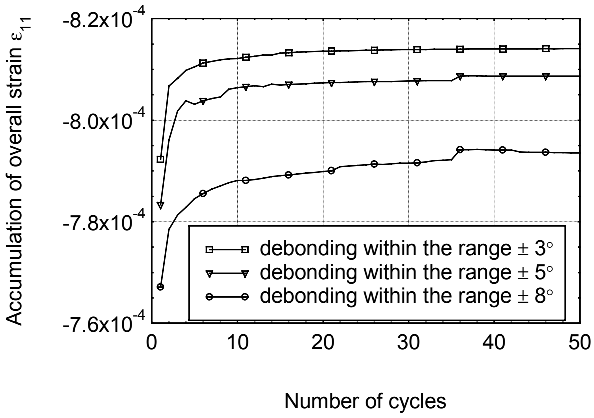

Fig. 6. Accumulation of the permanent overall strain ε_{11}, with microcracking in the matrix

However, if the whole matrix/inclusion interface were modelled as an ideal connection, than microcrack would not open at the interface and, consequently, crack tip would occur at the interface. The overall stress-strain curves calculated for the first 2 cycles is shown in Fig. 7.

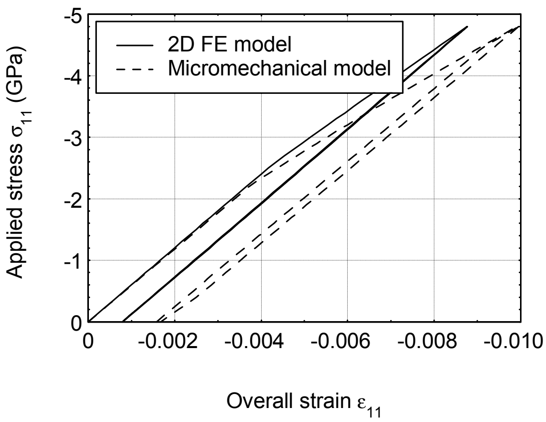

Fig. 7. Predicted overall stress-strain curves, microcracking in the matrix

By comparison with the micromechanical model it follows that the 2D finite element model is stiffer in the elastic-plastic range and predicts the half-permanent overall strain than that predicted by the micromechanical model. There is a quite good agreement in the overall yield stress values.

Ad 2a)
The FE model with the loading direction containing an angle of 45° with the principal direction of square array is much more compliant than the FE model with the loading direction parallel to the square array principal axis. Fig. 8 illustrates the overall stress-strain curves calculated for the

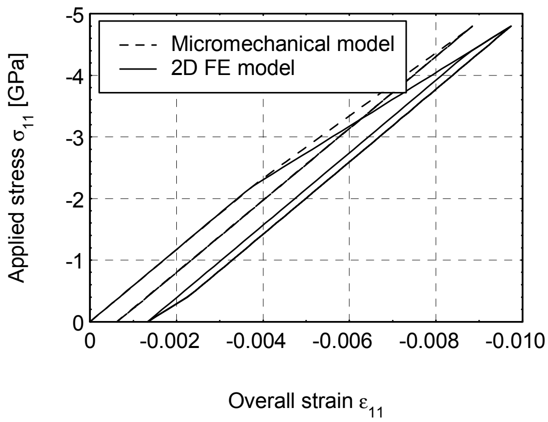

Fig. 8. Predicted overall stress-strain curves, no microcracking in the matrix

first 2 cycles. By comparison with the micromechanical model it follows that the 2D finite element model is more compliant within the elastic-plastic range than the micromechanical model

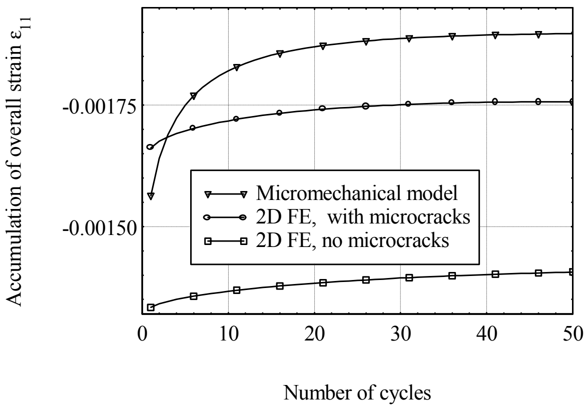

Fig. 9. Accumulation of the permanent overall strain ε_{11}

but provides an excellent agreement in the overall yield stress. Surprisingly, the accumulation of the permanent overall strain occurs even when no microcracks are present, see Fig. 9, the bottom curve. Such a kind of behaviour is caused by the character of residual stresses arising in the case of a diagonal arrangement of inclusion's square array and the loading direction. Specifically, upon unloading the residual stresses arising in the matrix between inclusions aligned with the loading direction are tensile while the residual stresses arising in the matrix between inclusions lined up perpendicularly to the loading direction are compressive. Hence, due to the synergism of both fields there may be achieved a sufficiently high level of the effective stress inside inclusions to initiate the backward plastic flow, which is necessary (but not sufficient) condition for the cyclic creep to occur. The inception of the backward plastic flow is quite apparent in Fig. 8. It should be emphasised however, that this behaviour is closely related to the specified geometry of the periodic inclusions' arrangements and loading direction.

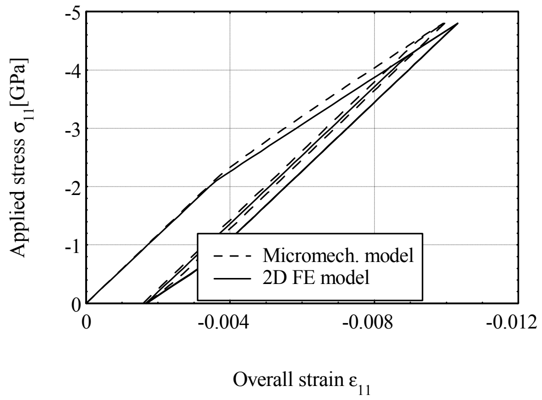

Fig. 10. Predicted overall stress-strain curves with microcracking in the matrix

Ad 2b)
Fig. 9 indicates that the presence of microcracks increases the accumulation of the permanent overall strain. The accumulated permanent overall strain computed using FEM is in this case in a good correspondence with that predicted by the micromechanical model. Fig. 10 shows a remarkable agreement of the overall stress-strain curves predicted for the first 2 cycles by the FEM and the micromechanical model. Nevertheless, further computations are needed for to confirm that this agreement is rather not coincidental.

SUMMARY

FE element results presented confirm the conclusions, made previously basing upon the micromechanical model [1], that the microcracks nucleated at the inclusion/matrix interface and extending in the direction parallel to the pressure loading direction significantly influence the resulting overall response of the brittle matrix composite under cyclic pressure loading with nonzero mean stress. It was shown that matrix microcracking stimulates ratchetting of composite though the isotropic hardening rule for inclusions is used. As a next step in the analysis a cycle by cycle growth of microcracks will be assumed. It is expected that this analysis provides us with damage criteria suitable for metal particulate-reinforced brittle matrix composites subjected to cyclic compression loading.

Acknowledgement – The support of the Grant Agency of the Czech Republic through the grant No. 101/99/0829 is gratefully acknowledged.

REFERENCES

[1] Kotoul, M., A Micromechanical Modelling of Cyclic Creep in Brittle Matrix Composites under Compressive Loading, Proc. of MSMF-3, Brno, Czech Republic, 2001.